Scilight

Parasitological Science

https://www.sciltp.com/journals/parsci

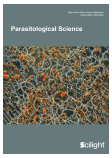

Article

In-Silico and Functional Characterisation of Nematode Galectin-3 and Galectin-9

Elizabeth Mullens [1], Gemma Zerna [2], Farah Ahmady-Nield [1,3], Travis Beddoe [2], David Piedrafita [4] and Sarah Preston [1,*]

[1] Institute of Innovation, Science and Sustainability, Federation University, Mount Helen, VIC 3353, Australia
[2] Department of Ecological, Plant and Animal Science, School of Agriculture, Biomedicine and Environment, Latrobe University, Bundoora, VIC 3083, Australia
[3] Fiona Elsey Cancer Research Institute, Ballarat Central, VIC 3350, Australia
[4] Institute of Innovation, Science and Sustainability, Federation University, Churchill, VIC 3842, Australia
* Correspondence: sj.preston@federation.edu.au

How To Cite: Mullens, E.; Zerna, G.; Ahmady-Nield, F.; et al. In-Silico and Functional Characterisation of Nematode Galectin-3 and Galectin-9. *Parasitological Science* **2025**, *1*(1), 4.

Received: 3 November 2025
Revised: 28 November 2025
Accepted: 4 December 2025
Published: 19 December 2025

Abstract: The search for novel treatments for chronic inflammatory conditions has led to an increased interest in gastrointestinal nematodes and the molecules they produce to evade the human immune system. Galectins are carbohydrate-binding proteins that are potent, multifunctional signalling proteins for the immune system, and form a large component of the excretory/secretory molecules nematodes produce during infection. The aim of this research was to determine if *Necator americanus* (New World Hookworm) and *Trichuris trichiura* (Human Whipworm), produced functional galectin homologues of human galectin-3 and -9 which interacted with host cells. Protein databases for *N. americanus* and *T. trichiura* were analysed for significant sequence and structural similarity to human galectin-3 and -9. Four proteins were expressed using *Escherichia coli* (*E. coli*) and purified by lactose affinity purification. Recombinant Hookworm-galectin-3 (rHW-gal-3) was capable of agglutinating horse red blood cells (RBCs) at >59.5 µg/mL, and increased proliferation in the human epithelial HCA-7 CRC colon carcinoma cell line, at test concentrations >1.25 µL/mL, compared to untreated cells (p-value < 0.05). Recombinant Whipworm-galectin-9 (rWW-gal-9) binding was visualised on HCA-7 CRC cells but had no-effect on proliferation. Recombinant Whipworm-gal-3 (rWW-gal-3) and Hookworm-gal-9 (rHW-gal-9) did not bind or significantly alter the proliferation of HCA-7 CRC cells but possessed carbohydrate binding evidence through lactose affinity purification. *In-vitro* results suggest that synthetic nematode galectin molecules, selected through in-silico comparison to human galectin-3 and galectin-9, had carbohydrate binding activity, and that some were capable of binding and interfering with host cell processes. This research furthers our understanding of nematode-host interaction.

Keywords: galectin-3; galectin-9; nematode; homology; bioinformatics

1. Introduction

Chronic inflammation occurs when proinflammatory cytokines and immune cells remain active in the body for extended periods of time, without resolution of inflammation and tissue repair [1]. Chronic inflammation contributes to approximately 50% of deaths worldwide [2]. Chronic inflammatory conditions are usually treated with non-selective cyclooxygenase (COX) inhibitors however, long term use of non-steroidal anti-inflammatory drugs (NSAID), can cause liver and renal toxicity [3,4]. Hence, safer anti-inflammatory drugs are needed to treat inflammatory diseases. Molecules released by gastrointestinal nematodes (GIN), may be novel treatment options

for these conditions, by exploiting the co-evolution of parasites within host systems, to create safer anti-inflammatory drugs for long term use [5].

Gastrointestinal nematodes (GIN) can regulate host immunity by down-regulating T-helper 2 (Th2) inflammatory responses to promote their own survival [6,7]. The immune response to GIN infection is driven by the Th2 response, early response is characterised by increases interleukin-4 (IL-4), IL-5, IL-9 and IL-13, whereas persistent Th2 response to parasite infection is marked by an increase in IL-10 and transforming growth factor beta (TGF-β) [8]. Live worm trials in humans, to verify the effectiveness of GINs for treatment of chronic inflammatory diseases have reported some positive results. In coeliac patients following controlled *Necator americanus* infections, researchers observed expansion and induction of T-regulatory cells (T_{reg}), which promote tolerance of self-antigens and inhibit inflammatory responses of other immune cells, and tolerance to gluten challenge [7,9,10]. Pig whipworm, *Trichuris suis,* has also been used in human trials for the alleviation of inflammatory conditions [7].

Molecules produced and released by GIN downregulate inflammation [11]. Previous studies on excretory/secretory (ES) products from GIN have identified many immune-modulatory molecules. ES-62 from *Acanthocheilonema viteae,* macrophage migration inhibitory factor (MIF) and *Toxascaris leonina*-galectin-9-homolog are some ES products that have been examined in *in vitro* and animal models [12–15]. Investigation of the mechanisms of immune regulation by live GIN may assist in the design of new anti-inflammatory drugs.

Galectins are proteins that bind to β-galactosides [16] and they are found in mammals and secreted by helminths [17]. Galectins bind sugars through the carbohydrate recognition domain (CRD), a conserved region of β-pleated sheets [18]. Two galectins of particular interest to this study are human galectin-9 (gal-9) and human galectin-3 (gal-3). These galectins may play a role in mast cell regulation, key effector responses against nematode infections, but they are also important in anaphylaxis, and T-helper (Th) differentiation [19–21].

Human gal-9 is generally characterised as an anti-inflammatory molecule, promoting T_{reg} differentiation and survival along with inducing apoptosis in Th1 cells [21,22]. Human gal-9 drives dendritic cells towards promoting a prolonged Th2 response, which is linked to food allergy responses [23]. Gal-9 is a tandem-repeat galectin, with two unique carbohydrate recognition domains (CRDs) [24,25].

Human gal-3 is a chimeric galectin; it contains one CRD and a tail-like structure [26]. It is prevalent throughout many body systems, and highly expressed by myeloid, epithelial and endothelial cells and fibroblasts [27]. Gal-3 can exist in single units or as oligomers [28]. Human Gal-3 has the ability to facilitate IgE cross-linking, which is required in mast cell degranulation in response to nematodes and allergens [29,30].

Nematode galectins have been found highly abundant in ES products and galectin expression is widespread among nematodes [31]. Additionally, ES proteins from *Trichinella spiralis* that are "galectin-like" have been found to promote dendritic cells to polarise naïve T cells into a regulatory state [32]. Hafidi et al. demonstrated that nematode galectins from *Teladorsagia circumcincta* could bind a large variety of host proteins. Furthermore, nematode galectin could restrict mast cell degranulation by binding available IgE glycosylation sites and prevent cross-linking with mast cells [17]. *T. circumcincta* galectin (*T. circ*-gal-1) could inhibit mast cell degranulation [30]. Possibly due to gal-3 polymers facilitating the crosslinking of IgE needed for mast cell degranulation due to their identical binding sites, when in a polymerised structure [30]. This leads to the hypothesis that parasite galectins like *T. circ*-gal-1, which are tandem galectins with different CRDs, could inhibit IgE crosslinking on mast cells, supporting nematode galectins as immunomodulatory molecules [30,33].

The aim of this paper is to determine if galectins from human helminths, *N. americanus* and *T. trichiura*, have similar galectins to human galectin-3 and 9, that could be examined to assess for immunomodulatory effects. We used bioinformatic characterisation to select possibly candidates, generated recombinant molecules and assessed their ability to interfere with epithelial cells.

2. Methods

2.1. Selection of Nematode Galectins

A bioinformatic pipeline was derived and followed to select appropriate nematode galectins for synthesis. The first step was sequence retrieval (A), then determination of conserved binding sites from human galectins, sequence alignment and conserved binding site analysis (B and C), phylogenetic analysis of sequence, pairwise alignment, and finally structural matchmaking (D). A summary of the workflow is represented in Figure 1 and further details are below.

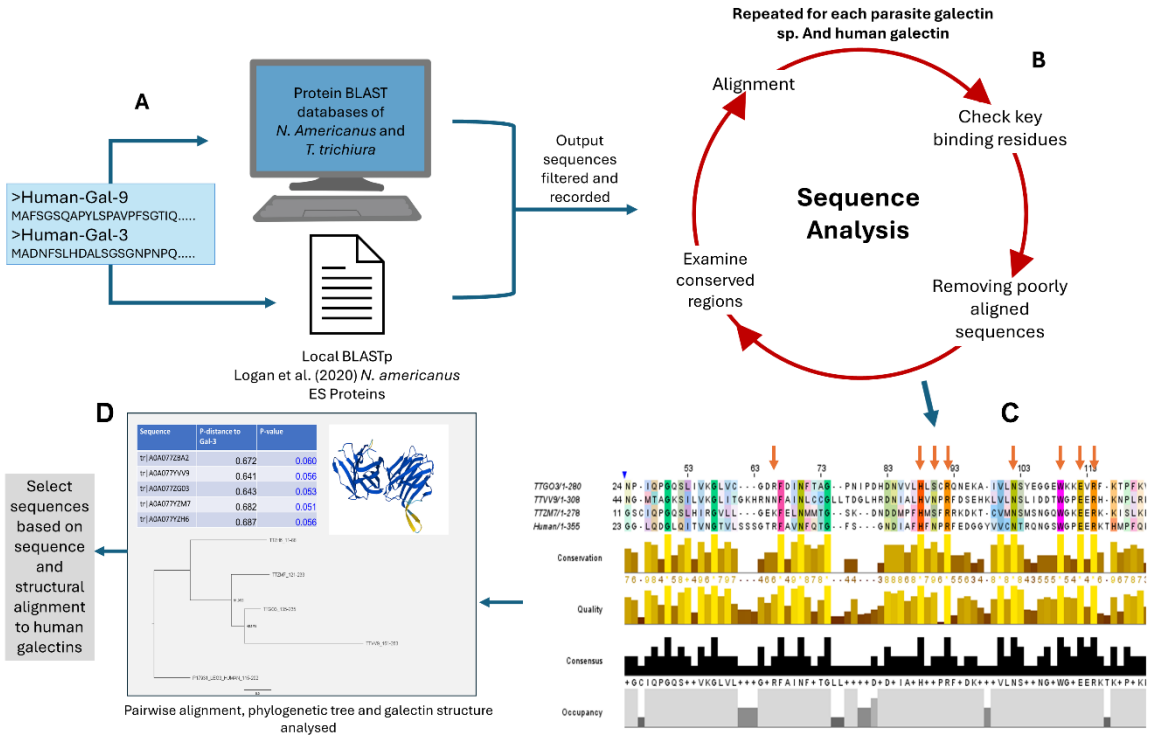

Figure 1. Bioinformatic methods for the selection of nematode galectins. Nematode galectin sequences were mined using two Basic Local Alignment Search Tool (BLAST) programs and a keyword search. Human galectins 9 and 3 were used as templates to find similar sequences in the proteomes of *Necator americanus* and *Trichuris trichiura* [34] (**A**). Each grouping was analysed to determine four galectin candidates for this study. The amino acid sequences were first aligned (**B**) and key binding residues checked (**C**). The remaining sequences were compared through pairwise alignment, phylogenetic tree analysis and predicted structure (**D**).

2.2. Protein Sequence Acquisition for Nematode Gal-3 and Gal-9

Human gal-3 (Acc#: P17931) and gal-9 (Acc#: O00182) amino acid sequences were used as templates in a Basic Local Alignment Search Tool (BLAST) search to identify similar protein sequences in *T. trichiura* [35] and *N. americanus* [36] (Figure 1). Three different databases were used; National Center for Biotechnology Information (NCBI) protein database, UniProt and a local database for the proteome of *N. americanus* [34]. Sequences were acquired from the NCBI (NCBI; http://www.ncbi.nlm.nih.gov/ (accessed on 5 May 2022) [37] and UniProt [38] databases, using a BLAST search, followed with a keyword search, both limited to the target species, *N. americanus* and *T. trichiura*. Sequences were also collected from keyword searches "galectin" and "parasite name" on UniProt [39]. Further, Logan et al. released their paper "Comprehensive analysis of the secreted proteome of adult *N. americanus* hookworms", the sequences were downloaded from the online repository for local BLAST+ [40]. The protein sequences that were analysed are recorded in Supplementary Materials. Due to the low number of sequences for each query, all results were retained and cross referenced to remove any duplicates across the acquisition methods.

2.3. Bioinformatic Analysis of Protein Sequences and Comparison of Human Galectin-3 and -9 to Nematode Galectins

The selected protein sequences were imported into MEGA11 (v 11.0.11) [41] and aligned using Multiple Sequence Comparison by Log-Expectation (Muscle) with default settings. The aim of this step was to filter out sequences to candidate sequences for gal-3 or gal-9 homologues from each nematode species. This step was conducted in four separate alignments, two from each nematode species, which would each be aligned to human gal-3 and gal-9. Each of the following steps were applied to these sequence groups individually. Aligned sequences that were too long, short, duplicates or lacked key binding residues were removed, and the remaining sequences were aligned again, and imported into Jalview (v 2.11.2.6) [42] to assist in visualisation. The alignments were coloured by conservation using a 30% similarity threshold to highlight conserved residues. The conserved binding residues for human gal-3 and gal-9 are in Table 1. The full protein sequences and BLAST output statistics are recorded in the Supplementary Materials.

Table 1. Key binding residues of human galectin-3 and galectin-9.

Galectin/CRD	Carbohydrate Binding Region	Key Binding Residues	Reference
Gal-3/CRD	P^{113}-I^{200}	R^{144}, H^{158}, N^{160}, R^{162}, N^{174}, W^{181}, E^{184}, R^{186}	[26]
Gal-9/N-CRD	G^{23}-Q^{121}	R^{43}, H^{60}, N^{62}, R^{64}, N^{74}, W^{81}, E^{84}, R^{86}	[24]
Gal-9/C-CRD	V^{200}-I^{339}	R^{221}, H^{223}, N^{225}, H^{235}, N^{237}, R^{239}, N^{248}, I^{251}, D^{252}, N^{253}, S^{254}, W^{255}, E^{258}, R^{302}	[25]

The alignments were saved in triplicate, and alignments were trimmed to the binding region of the human galectin (gal-3, N-terminal gal-9, C-terminal gal-9), to account for similarity in the binding region (Table 1). Parasite galectin *T. circ*-gal-1 was previously researched by Donskow-Łysoniewska et al. [17] and was found to have immune regulating activity in mast cells. This was also aligned with the parasite galectins to assist in choosing sequences downstream.

After initial processing in MEGA11, the alignment was imported into Jalview to visualise, trim the alignment, and create FASTA files for future processing. To make phylogenetic trees for comparisons, alignments were imported into IQ-tree (v 3.0) on the webserver (http://iqtree.cibiv.univie.ac.at/ (accessed on 1 September 2022); each alignment was then modelled using the find best model function, although for later runs ModelFinder in IQ-tree was used [43], the program was run under ultrafast bootstrap [44]. Each alignment was then used to make a phylogenetic maximum likelihood tree using the best model setting with IQ-tree [45,46]. Next, pairwise alignment was done for both the extended alignments and the binding region to determine the percentage similarity between sequence residues and the human galectin templates. The pairwise alignment was measured in p-distance (the percentage of amino acid substitutions between two sequences). Protein structure, as predicted by Alphafold [47], was used to determine if an amino acid sequence was likely transcribed correctly and complete, as well as if the secondary structure contained complete β-pleated sheets of galectin CRDs.

The galectin models of human gal-9, gal-3 and the nematode galectins of interest were imported into ChimeraX (v 1.7) [48]. This study used the AlphaFold supplied models from UniProt [39] and also the AlphaFold (v 2.3.0) modelling tool supplied in ChimeraX to model sequences [34]. AlphaFold was preferred as it retained all residues rather than trimming out disordered regions. The key binding residues were examined and coloured by which region of the human galectins they most closely aligned to. The tandem galectins were cut in the linker region to account for variation. The Matchmaker function in ChimeraX was used to align the CRD of human galectins to the CRD of nematode galectins to determine if the structure of the β-sheets of the CRD region was well aligned and the key binding residues in the same regions. A final proteome BLAST search was performed on each candidate sequence to determine if similar galectins had been recorded across other species. Comparable sequences were aligned in MEGA11 to confirm the length and accuracy of the candidate sequence. Based on these *in-silico* results four sequences were selected for protein expression and denoted as recombinant-Hookworm-galectin-3 (rHW-gal-3), recombinant-Hookworm-galectin-9 (rHW-gal-9), recombinant-Whipworm-galectin-3 (rWW-gal-3), and recombinant-Whipworm-galectin-9 (rWW-gal-9).

2.4. Protein Synthesis

The selected protein sequences and corresponding genome sequences for homolog protein candidates were scanned for translation errors from genome sequences, transmembrane sequences, and disordered regions. The sequences were altered to facilitate protein production in *Escherichia coli* via codon harmonisation [49]. Region encoding for an N-terminal-hexa-histidine tag (6XHis-tag) was added to facilitate protein purification through Nickel-affinity chromatography and identification with Anti-6XHis-tag-antibodies. The gene sequences were synthesised and cloned into the pET-28a plasmid through the NdeI and XhoI restriction enzyme sites by Bioneer (Bioneer, Daejeon, South Korea). Recombinant protein synthesis was completed according to methods outlined in [50]. The modified pET-28 plasmid containing the sequences for N-terminal-6XHis-tagged nematode galectin was transformed into *E. coli* T7 LysY cells (New England Biolabs, Ipswich, MA, USA) and grown on Luria-Bertani (LB) (1% (*w*/*v*) tryptone, 0.5% (*w*/*v*) yeast extract, 0.5% (*w*/*v*) NaCl 1.5% (*w*/*v*) agar) plates with kanamycin (50 µg/mL), following the protocol in [50,51]. Single colonies were inoculated into LB broth for overnight growth at 37 °C and 225 rpm. Seed cultures were then diluted 1:100 into 400 mL of LB broth in 2 L conical flasks. Growth at 37 °C and 225 rpm occurred until an OD600 of 0.6 was achieved. Subsequently, expression was induced with the addition of 0.5 mM of isopropylthio-β-galactoside (IPTG), and incubation occurred for a further 16 at 21 °C and 225 rpm. Cells were harvested via centrifugation (6000× g 15 min) and resuspended in lysis buffer. A Tris based (10 mM Tris-HCl, 14 mM β-mercaptoethanol, 0.5 M NaCl) lysis buffer was used for rWW-gal-3 (Acc#. A0A077YZM7) (at pH 7.4), rHW-gal-9 (Acc#. NAME_06068) and rWW-gal-9 (Acc#. A0A077ZG03) (at pH 9), whereas a phosphate based (10 mM

Na_2HPO_4, 1.8 mM KH_2PO_4, 2.5 mM KCl, 137 mM NaCl, 14 mM β-mercaptoethanol, pH 8) lysis buffer was used for rHW-gal-3 (Acc#. W2T6P9_NECAM) [34,38]. Cells underwent a freeze-thaw cycle at −20 °C for a minimum of 4 h before being incubated with head-over-tail mixing with the addition of lysozyme (10 µg/mL). Samples were subsequently subjected to sonication (3 cycles of 30 s pulse, 30 s pauses) using a microtip and 35% amplitude. Cell lysate was clarified via centrifugation at 35,000× g for 20 min.

The supernatant was collected and purified using α-Lactose-Agarose resin (Sigma-Aldrich, Burlington, MA, USA, #L7634) according to Wu et al. [52], although employing a gravity flow column. Briefly, 1 mL of α-Lactose-Agarose resin suspension was added to 50 mL of bacterial lysate supernatant and incubated for 1 h at 4 °C. The resin and supernatant were added to a 10 mL gravity chromatography column. Up to 150 mL of wash buffer, the recipe changed based on the galectin type. Recombinant-Hookworm-gal-3 (rHW-gal-3) wash buffer (phosphate buffered saline (PBS), 14 mM β-mercaptoethanol, pH 7.4) and tandem-repeat-galectin wash buffer (PBS, 14 mM β-mercaptoethanol, and 0.03% CHAPS detergent, pH 7.4) were used to remove non-binding contaminants, aliquots were analysed using NanoDrop™ 2000 Spectrophotometer (Thermo Scientific, Waltham, MA, USA) and absorbance measured at 280 nm [52]. The rHW-gal-3 was eluted using the following buffer (PBS, 14 mM β-mercaptoethanol, 100 mM lactose, pH 7.4). The remaining galectins were eluted using a higher concentration of lactose (PBS, 14 mM β-mercaptoethanol, 200 mM lactose, pH 7.4). The elution was collected in 1 mL aliquots, sampled for SDS-PAGE and protein quantified using Nanodrop™.

To confirm purity and protein expression the flow-through, wash and elution fractions were run on 4–20% Mini-PROTEAN® TGX™ Precast Protein Gels (BioRad, Hercules, CA, USA, #4561093) according to the manufacturer's instructions and visualised using Bio-Safe™ Coomassie Stain (BioRad, #1610786). The eluted galectin fractions with target bands at the expected molecular weight, were concentrated using Amicon® Ultra Centrifugal Filter, 10 kDa molecular weight cut-off (Millipore, Darmstadt, Germany, #UFC9010). Final concentration was determined using NanoDrop™, then diluted to ~0.5 mg/mL. Half of the yield was passed through Pierce™ High-Capacity Endotoxin Removal Spin Columns (Thermoscientific, #88274) according to the manufacturer's instructions and the concentration was remeasured, and samples were assessed on SDS-PAGE, before freezing all aliquots to −80 °C [52]. Three different batches of the 4 nematode galectins were produced and used in assays.

Before use protein was thawed and desalted using Amicon® Ultra Centrifugal Filter (10 kDa cut-off), by washing with 10 mL sterile PBS (pH 7.4) and centrifuged at 3750× g for 15 min twice, then washed once more, centrifuging for 25 min. The protein concentration was determined using a Pierce ™ Bradford Plus Protein Assay Kit (Thermo Scientific, Cat. #23236).

2.5. Proliferation Assay

The culturing of human colorectal cancer (HCA-7 CRC) cell line has been described previously with the following alterations [53]. Briefly, HCA-7 CRC cells were maintained in Complete Roswell Park Memorial Institute (RPMI) media (10% foetal bovine serum (FBS) (Gibco, Grand Island, NY, USA), 1% Pen/Strep Mix, 1% Glutamax (Gibco)) and cultured at 37 °C and 5% CO_2. Cell cultures were passaged in T75 flasks, every 4–6 days or at 70% confluence, by detaching with Trypsin/EDTA (Gibco), and seeding at 4×10^4 cells/cm^2.

For proliferation assays, cells were seeded into sterile 96-well flat-bottom plates at a density of 1×10^3 cells per well, reserving three wells of media only as the spectral blank. A second plate was set up likewise with only six wells of cells as a 0-h control and allowed to attach under normal culture conditions for 24 h at 37 °C and 5% CO_2. A dilution of parasite galectin in complete RPMI media was made to 10 µg/mL and passed through a 0.22 µm pore polyethersulfone syringe filter (Millipore, Burlington, MA, USA, #SLGPR33RS). 10% dimethyl sulfoxide (DMSO) was used as a negative, no cell growth control. The controls were plated in triplicate. The parasite galectin was plated in a 1:2 serial dilution from 5 µg/mL to 0.078 µg/mL, this was repeated for a total of six replicates per plate. For the 0-h plate 10 µL of 3-(4,5-Dimethylthiazol-2-yl)-5-(3-carboxymethoxyphenyl)-2-(4-sulfophenyl)-2H-tetrazolium (MTS) reagent was added to each well and the plate was returned to incubation at 37 °C and 5% CO_2 for 1.5 h, before reading at 490 nm on a plate reader. The plates were incubated for 24, 48 and 72 h at 37 °C and 5% CO_2 for the initial experiments, at the required time point, the plate was removed and 10 µL of MTS reagent was added to each well and the plate was incubated for 1.5 h at 37 °C and 5% CO_2, before reading on a plate reader at 490 nm. Subsequent experiments were read at 24 h only.

2.6. Localisation of Endogenous Galectin and Parasite Galectin in HCA-7 CRC Cells

To visualise if parasite galectin was binding to the HCA-7 CRC cells, the cells were cultured for 72 h in Nunc™ Lab-Tek™ Chambered Cover glass (Thermo Fisher, MA, USA, #155411PK) slides at 37 °C and 5% CO_2, in complete RPMI with 10 µg/mL of nematode galectin. Cells were fixed with 10% formalin for 10 min. The

formalin was removed, and the cells were washed 3 times for 5 min with PBS. The cells were then covered with PBS and refrigerated to 4 °C before staining. The following incubations were performed at room temperature (RT) on a shaking platform. Cells were blocked with a blocking buffer of 1% bovine serum albumin (BSA) in PBS for 1 h at RT. The anti-6XHis-tag-FITC antibodies (Thermo Fisher, #A190113F) were diluted 1:3000 in 0.1% BSA blocking buffer. The slides were incubated in the dark for 1 h at room temperature, washed, for 5 min, 3 times with PBS, being sure to keep cells in the dark or wrapped in foil. Drops of DAPI mounting medium were applied and the cells were visualised using Nikon Eclipse Ti2 confocal microscope and NIS-Elements software. The images were compiled and processed using FIJI ImageJ (v 1.54p) to measure the mean grey value of each cell. The data from each colour channel was analysed in RStudio [54].

2.7. Haemagglutination Assay to Confirm Carbohydrate Binding

Hemagglutination assays were performed to confirm carbohydrate binding of the nematode galectins according to Prato et al. [55]. Briefly, 100 µL of defibrinated horse blood was mixed with 1 mL of PBS and centrifuged at 2200× g for 15 min at 4 °C, the supernatant was discarded and the pellet was mixed with 960 µL of PBS + 1% BSA [55]. Serial dilutions of 1:2 of the galectins in PBS-BSA were made in a 96-well plate for a final volume of 50 µL, including control wells.

This was performed for nickel-purified galectins in concentrations of 120–0.23 µg/mL for rHW-gal-3, rWW-gal-3, and rHW-gal-9, and 60–0.12 µg/mL for rWW-gal-9.

Lactose-purified galectin concentrations ranges were, 119.5–0.8 µg/mL of rHW-gal-3; 65.5–8.2 µg/mL of rWW-gal-3 and ~237.5 µg/mL of rHW-gal-3 in storage buffer. Finally, 50 µL of horse red blood cell (RBC) suspension was added, mixed and incubated for 1 h at RT before visualising for agglutination [55].

Only lactose-purified rHW-gal-3 was used for replicate analysis following haemagglutination results.

2.8. Data Analysis and Statistics

Data analysis and statistics were conducted in R using RStudio v. 4.3.2 [56], and the following R packages were used: ggbreak v. 0.1.4 [57], ggpmisc v. 0.6.2 [58], ggpp v. 0.5.8.1 [59], ggpubr v. 0.6.0 [60], ggtext v. 0.1.2 [61], knitr v. 1.48 [62], openxlsx v. 4.2.8 [63], plotrix v. 3.8.4 [64], rmarkdown v. 2.27 [65–67], rstatix v. 0.7.2 [68], standard v. 0.1.0 [69], tidyverse v. 2.0.0 [70]. Proliferation and localisation data was analysed in RStudio. For localisation and proliferation assay datasets normality was determined using histograms in ggplot and a Shapiro-Wilk normality test (rstatix). Significance of the proliferation assay was determined using a paired Wilcoxon signed-rank test in reference to the respective control group. An unpaired *T*-test was used to determine the significance of galectin localisation in cells relative to the control group. Graphs were produced using the package ggplot. Differences between groups were considered statistically different if the p value was less than 0.05.

3. Results

3.1. Sequence Retrieval, Filtering, and Analysis

In total, 8 unique galectin-like sequences were acquired from *T. trichiura,* and 23 unique sequences were acquired from *N. americanus*. For *T. trichiura* and *N. americanus*, the sequence results were analysed for similarity to both human gal-9 and gal-3, and a single candidate sequence was chosen for each based on similarity of key binding regions and similarity of secondary structure (detailed outputs in Supplementary Materials). These sequences are presented in Table 2. Sequence rHW-gal-3 is a prototype galectin with a single CRD, while the remaining sequences are tandem galectins.

Table 2. Nematode sequences selected for further analysis. The sequence rHW-gal-9 was trimmed and the region to the amino acid M^{97} was removed after visually assessing the predicted secondary structure and sequences that returned high sequence homology following BLAST search.

Human Galectin	Nematode Galectin	Homologue Sequence Name (UniProt Acc. #)	Abbreviation	Amino Acid Sequence
Galectin-3	*T. trichiura*	TTZM7 (A0A077YZM7)	rWW-gal-3	MSVPYLSRLEGSCIQPGQSLHIRGVLLGEKFELNMM TGSKDNDDMPFHMSFRRKDKTCVMNSMSNGQWGK EERKKISLKENEPFDLRIRAHDSKFEVFLNQKELCEY DYRQPLTSISFIRINGDVELNHVSWGGKYYPVPYEAG IPDGFSPGKRLYVSGVPEKKAKRFAVNILTSSGDIALH FNVRFDEKVRCRAVVLFNTIVRNSQFGGTWQNEERE GKLTLEKDHAFDLMFVNEVHSFQVFINGIHWCAYAH RTDPNSLKGLRIEGDVELQGVHVK

Table 2. *Cont.*

Human Galectin	Nematode Galectin	Homologue Sequence Name (UniProt Acc. #)	Abbreviation	Amino Acid Sequence
Galectin-3	*N. americanus*	NA521 (W2T6P9)	rHW-gal-3	MIGAGVGMGPSPVLYNSATPAGLRFAGFENGKRLRL VLIPLPEGNKFAVNFRTPYDIAFHFNPRFDEDCVVSNS TRNGGWLNEERTNNPFQVGKVYTVEFVSNYGQIQV LLNGVPFTTFAERLPGHDINSVEVEGGVHVHSAHVF
Galectin-9	*T. trichiura*	TTGO3 (A0A077ZG03)	rWW-gal-9	MLTTAEDLHKEWMKKLPYWAKLENPIQPGQSLIVK GLVCGDRFDINFTAGPNIPDHDNVVLHLSCRQNEKAI VLNSYEGGEWKKEVRFKTPFKVGEPFDVRIRAHDD RYEIFADHKHLGDFKHRLALTATTHVNIQGQCEVNA VLWEGNYYSVPYKTSITGFAPGRRLFVSGIAVDSPKR FAVNFFSKDDIALHFNVRFDEKKVVRNTLKGGAWG KEDRVGGFPFEKKKNFDLLFVCEEDTIQIYINDDHFC HYAHHIPPKQIDAVEIEGDIELQLIHIE
	N. americanus	NALOG1 (002099269E)	rHW-gal-9	MVRLARSKSTVSVKSAVLSVKLPQHLQNSMTEKSY VSSFYLISGHGLQVYQVFRAALTATSANSRGKAPYSG HFRGRSAHLRSPQPALVVLDVSSRMPTLWHFAKYINI PYRSKLTEKIEPGQTLIIRGRTSEEAKRFNINLHKDSP DFSGNDVPLHVSVRFDEGKLVFNSYTKGAWGKEER QKNPVKKGDGFDIRIRAHDNKFTVSINRKEVKSFEH RIPLQHVTHLSIDGDVVLNHVQWGGKYYPVPYESGI AENGLIPGKTLVIYGTPEKKAKKFNINLLKKNGDIAL HFNPRFDEKAKGFICGKIKPGCVIRNSLVNGEWGNEE REGKNPFEKGVGFDLEVKNEEYAFQIFVNGERFASY AHRIDPHEIGGLQIHGDVELTGIQIVGN

3.2. Galectin Visualisation and Analysis

3.2.1. Galectin-3 Homolog from Hookworm (*N. americanus*)—rHW-gal-3

Twenty-three sequences were retrieved from *N. americanus* (Supplementary Materials), 11 sequences contained >85% similarity of the key binding residues in the CRD (Figure 2). Pairwise alignment indicated that only one sequence had a binding region significantly similar to human gal-3, W2TY78_NECAM (*p*-distance = 0.746, standard error = 0.047). However, the maximum likelihood tree modelled the binding region of rHW-gal-3 (W2T6P9), slightly closer to human gal-3 than W2TJZ4_NECAM and W2TY78_NECAM (Model: Blosum64 + G4, Bootstrap: 1000) (Supplementary Materials) [39].

The predicted structure of rHW-gal-3 also resembled a prototype galectin. rHW-gal-3, was modelled and the results of the Matchmaker function displayed that rHW-gal-3 had Lysine (Lys)^{46} in place of the Arginine (Arg) residue that would be present in human gal-3 (Arg^{144}) (Figure 2). All other key binding residues were predicted to be identical to the human gal-3 binding residues.

3.2.2. Galectin-3 Homolog from Whipworm (*T. trichiura*)—rWW-gal-3

For *T. trichiura* gal-3 (rWW-gal-3) homologue processing, 8 unique sequences were retrieved (Supplementary Materials), after alignment this was reduced to 4 based on sequence length and similarity to key carbohydrate binding residues. The 4 selected sequences were identical for >75% of the key binding residues. Galectin rWW-gal-3 was selected for further analysis before production (Figure 2). While it was not phylogenetically the closest to the template, human galectin-3, the binding region was most similar (*p*-distance = 0.670, standard error = 0.05).

The Matchmaker outputs for rWW-gal-3 are displayed in (Figure 2B). One key binding residue was different between the N-CRD of rWW-gal-3 and human gal-3, Serine (Ser)^{50} was substituted for Asparagine (Asp)^{160} (Figure 2). The C-CRDs of rWW-gal-3 and human gal-9 were also aligned in Matchmaker, a substitution of Alanine (Ala)^{169} for Histidine (His)^{255} and Isoleucine (Ile)^{251}, Aspartate (Asp)^{252}, Asn^{253}, Ser^{254} for Phenylalanine (Phe)^{208}, Glycine (Gly)^{209}, Gly^{210}, Threonine (Thr)^{211} was observed (Figure 3).

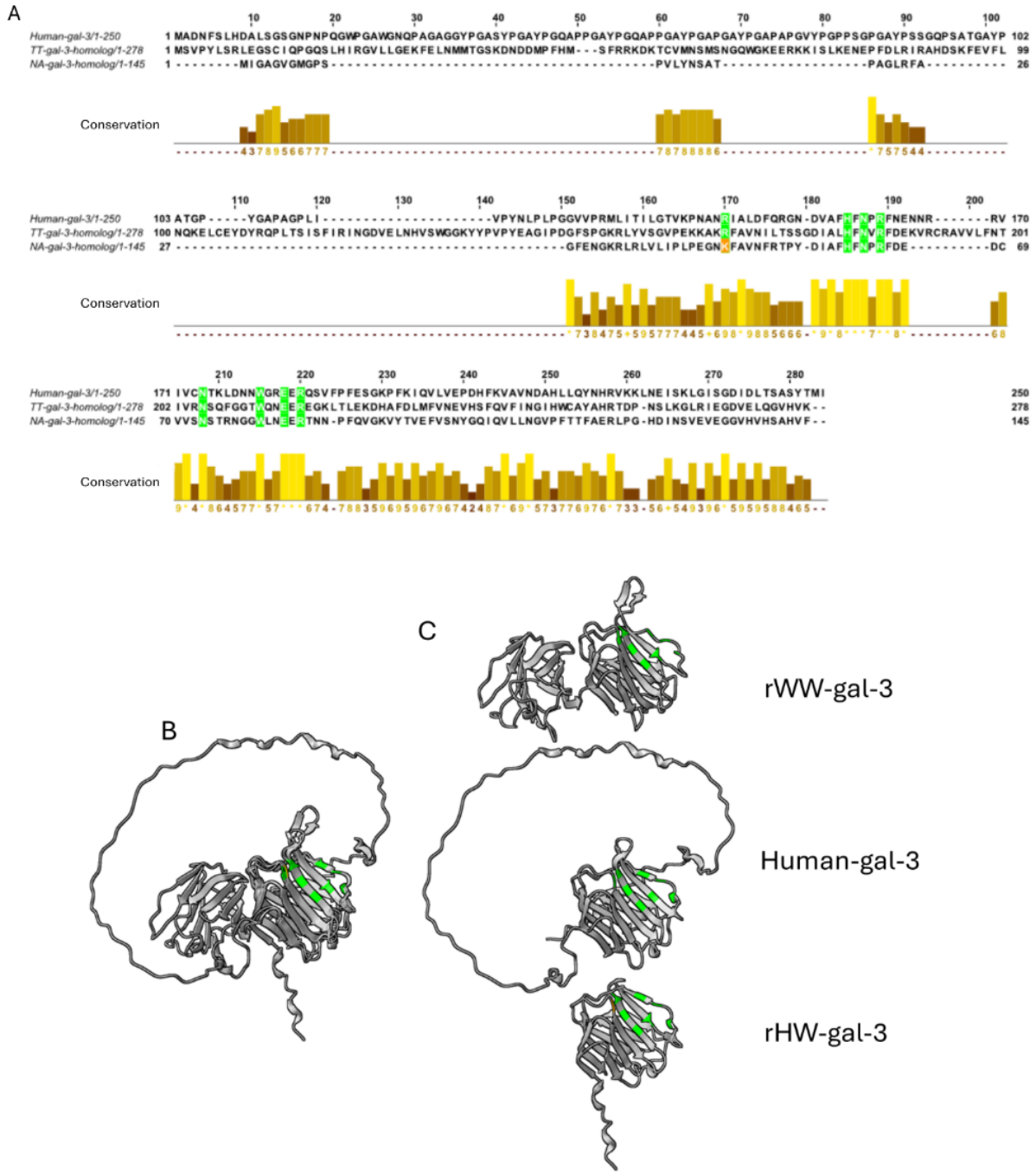

Figure 2. Sequence alignment of human gal-3 and nematode homologs and predicted models as aligned using Matchmaker outputs. (**A**) Conserved key binding residues (green), key binding residues not shared (orange). (**B**) Matchmaker overlay of human gal-3, rHW-gal-3, and Whipworm-gal-3-homolog (rWW-gal-3). (**C**) Separated view of rWW-gal-3, Human gal-3, rHW-gal-3. Key binding residues that aligned with human galectin (green) and substitutions (orange). The residue Lys^{46} is present on rHW-gal-3 where and Arg is present in the human model as shown in (**A**).

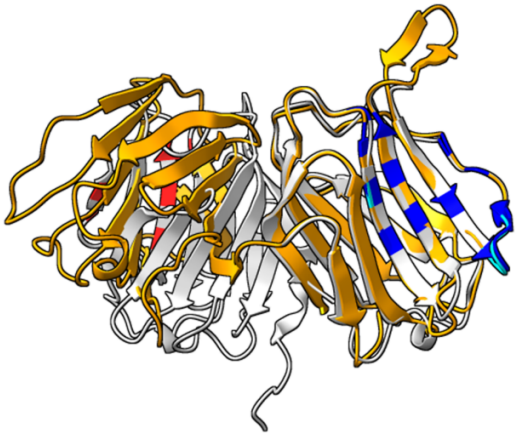

Figure 3. Structures of rWW-gal-3 (orange) and human-gal-9 C-CRD (grey) aligned in *Matchmaker*. Conserved C-CRD key binding residues (blue), N-CRD key binding residues (red) substitutions (cyan).

3.2.3. Galectin-9 Homolog from Hookworm (*N. americanus*)—rHW-gal-9

After the bioinformatic initial filtering steps, 10 sequences were retained with >75% similarity in key binding residues with human gal-9 N-CRD (Figure 4). Following analysis of sequences using pairwise alignment, it was determined that the N-CRD binding region of rHW-gal-9 was similar to human gal-9 N-CRD (*p*-distance = 0.687, standard error = 0.048). NAME_11043 (*p*-distance = 0.708, standard error = 0.047) and W2TVN3_NECAM (*p*-distance = 0.687, standard error = 0.047) were similar to human gal-9 at the N-CRD region [34,39].

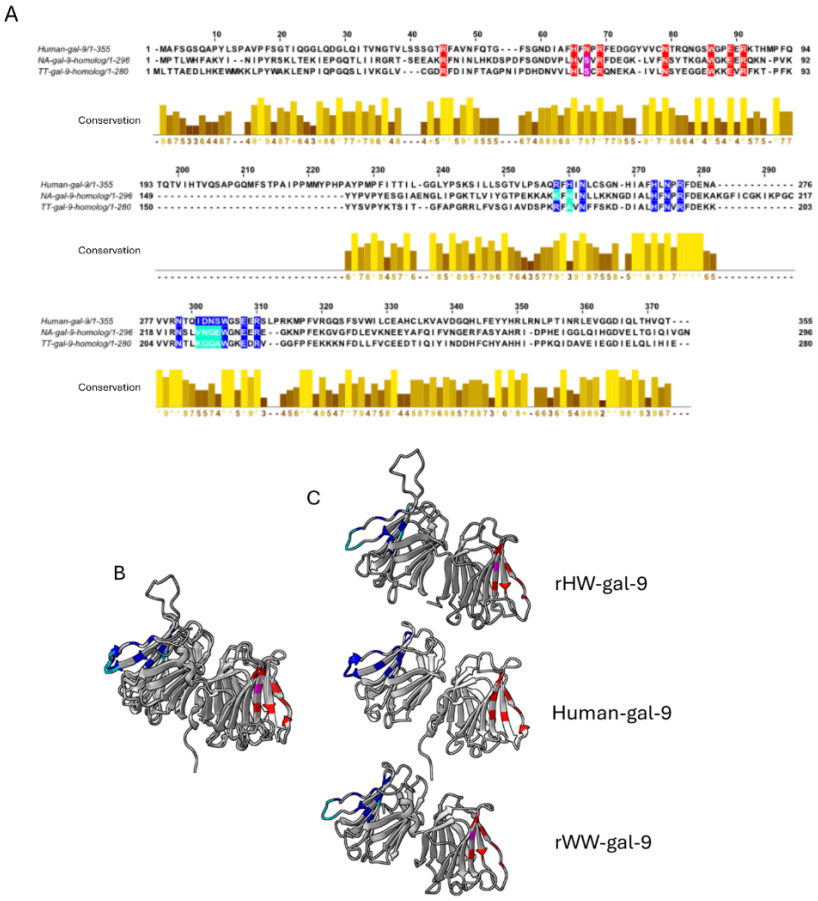

Figure 4. Sequence alignment of human gal-9 and parasite homologs and predicted structure and Matchmaker outputs. Conserved sequences of N-CRD (red) and C-CRD (blue), residues not shared in homologs (purple and cyan). (**B**) *Matchmaker* overlay of human gal-9, Hookworm-gal-9-homolog (rHW-gal-9), and Whipworm-gal-9-homolog (rWW-gal-9). (**C**) rHW-gal-9, Human gal-9 and rWW-gal-9, separated view. Key binding residues that aligned with human galectin N-CRD (red) and C-CRD (blue) and substitutions (purple and cyan) as shown by (**A**).

Sequence rHW-gal-9 was found to have a disordered region at the N-terminal, it was assumed that the start codon was incorrectly recorded. To determine if this was the case, a protein BLAST of rHW-gal-9 was performed, and the top 50 sequences were imported into MEGA11 and aligned. Once aligned the rHW-gal-9 sequence showed high similarity to other nematode galectins retrieved from BLAST and a pairwise alignment revealed most had 70–80% sequence similarity (Supplementary Materials). The protein was trimmed to the start codon Methionine (Met)^{97} (Table 2), which aligned with most of the sequences retrieved by BLAST, and re-modelled, as visualised in Figure 5.

This process was repeated with the rWW-gal-3, rWW-gal-9 and rHW-gal-3 but no other sequences were changed for the bioinformatic analysis. Compared to the other sequences, rHW-gal-9 had 20 sequences with high similarity (>85%) between different nematode species, whereas rWW-gal-3, rWW-gal-9 and rHW-gal-3 displayed a total of 3 sequences with >80% similarity (Supplementary Materials).

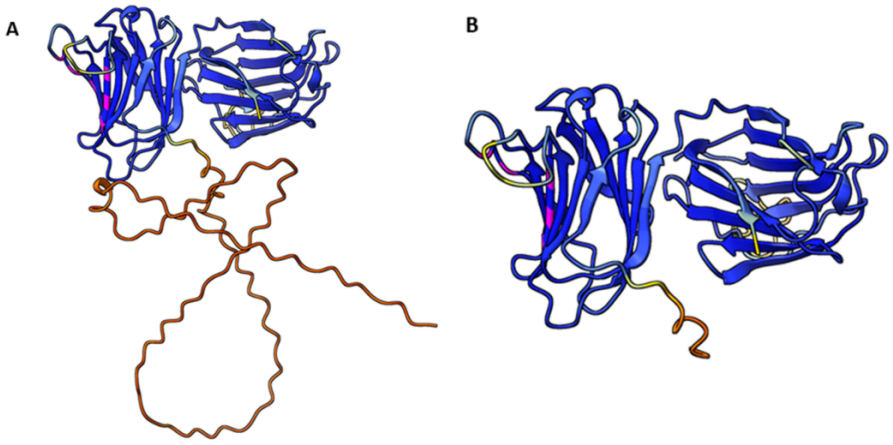

Figure 5. The structure of rHW-gal-9 as predicted by Alphafold. Before (**A**) and after removing disorganised region (**B**). The disorganised region (red) was removed to the amino acid M^{97}.

The AlphaFold models of human galectin-9 displayed low confidence values for modelling the linker region and can vary in length, therefore the structure of the N-CRD and C-CRD were analysed independently of each other. The structural model of rHW-gal-9 was separated into N-terminal CRD (Met^{1}-Tyrosine (Tyr)^{150}) and C-terminal CRD (Proline (Pro)^{151}-Asn^{392}). It was aligned with human gal-9, and the predicted protein structure of the sidechains were visualised. The results indicated that the predicted secondary structure of the binding regions, aligned with that of the human galectins. The N-CRD of gal-9 aligned slightly better than the C-CRD (Figure 4). rHW-gal-9 was also aligned with human gal-3, and it was determined through Matchmaker that human gal-3 aligned with the C-CRD of rHW-gal-9 (Figure 6). Of the eight key binding residues of the gal-9 N-CRD the only substitution was Ser^{63} in place of Asn^{62} (Figure 4). The gal-9 C-CRD alignment had two substitutions Lys^{181} (Asn^{253}) and Asn^{183} (His^{255}) and showed misalignment on one of the turns in the pleat structure (Figure 4C). The CRD of human gal-3 was also aligned in Matchmaker and aligned to the C-CRD of rHW-gal-9, with the only one key binding residue substitution, Lys^{181} (Arg^{144}) (Figure 6).

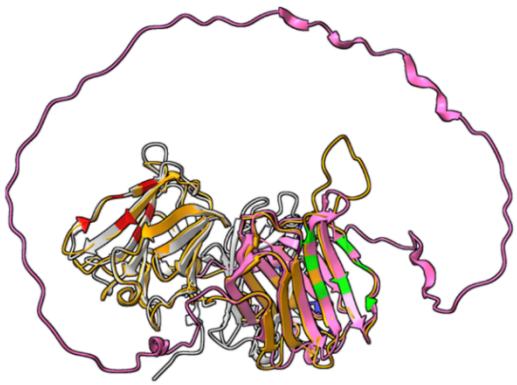

Figure 6. Secondary structure analysis of rHW-gal-9 (orange), gal-3 (pink) and gal-9 (grey) using Matchmaker. N-CRD key binding residues of gal-9 (red), substitutions (magenta) and C-CRD key binding residues (blue). Gal-3 key binding residues (green), substitutions (purple).

3.2.4. Galectin-9 homolog from Whipworm (*T. trichiura*)—rWW-gal-9

Eight sequences were retrieved from the *T. trichiura* proteome. After filtering, three sequences remained. These sequences contained >75% of the binding residues for human gal-9. Pairwise alignment showed that all three N-CRD binding region sequences were similar to the human gal-9 N-CRD (*p*-distance = 0.734, standard error = 0.046). The predicted secondary structure of all 3 parasite galectins suggested that these galectins were tandem in structure (Supplementary Materials). rWW-gal-9 was selected for further analysis using *Matchmaker,* after cleaving the protein in the linker region, the 2 CRD structures of rWW-gal-9 visually aligned with the CRDs of human galectin-9 (Figure 4C). Two key binding residues were different between rWW-gal-9 and human gal-9, Ser^{64} was substituted for Asn^{63} on the N-CRD and Ala^{182} for His^{255} in the C-CRD (Figure 4).

3.3. Recombinant Galectin Production

The T7 LysY *E. coli* cell line successfully expressed the recombinant proteins. Utilising Nickel-affinity purification, all four recombinant galectins were expressed and showed binding when a sample was passed over a lactose column however galectins produced using this method, produced inconsistent results between replicate assays. Lactose purification of bacterial lysate was employed to increase the amount galectin with active carbohydrate binding. SDS PAGE of fractions from lactose purification steps indicated that there was galectin present in the unbound flow-through for all galectins There was also galectin present in the eluted fractions, which indicated that a proportion of recombinantly expressed galectins bound to the lactose resin, suggesting carbohydrate binding capacity. The rWW-gal-3 eluted fraction displayed a band at ~52 kDa which is the predicted molecular weight of a galectin dimer. The eluted fractions post concentration (Figure 7) indicated low yield of rHW-gal-9 and rWW-gal-9 samples.

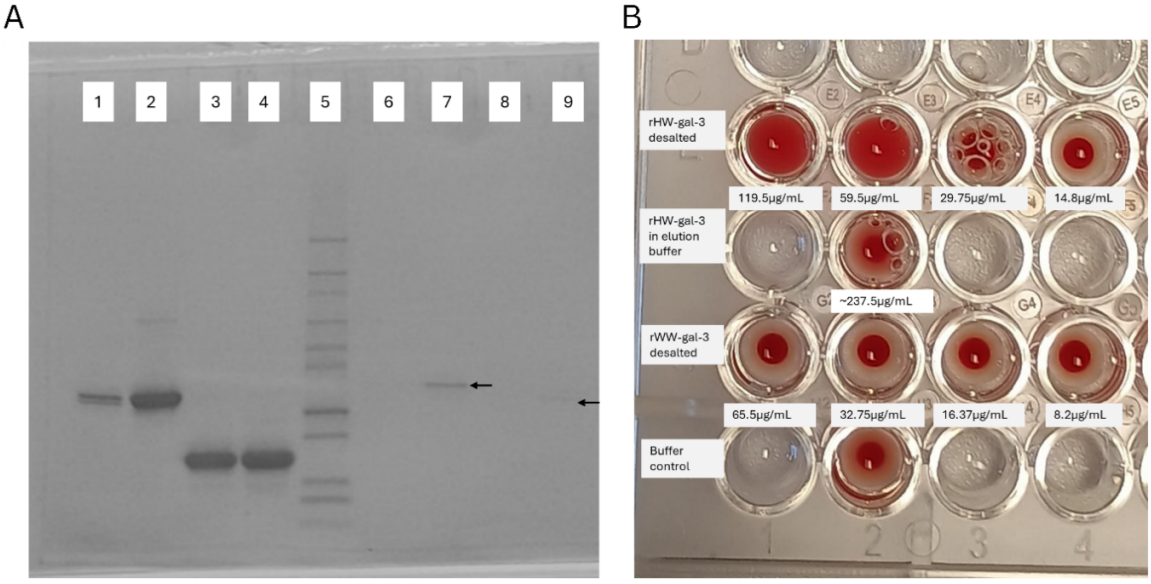

Figure 7. (**A**) Lactose purification and protein yields. Lactose binding fractions were pooled and concentrated. (1) rWW-gal-3 endotoxin removed (ER); (2) rWW-gal-3; (3) rHW-gal-3 (ER); (4) rHW-gal-3; (5) Ladder; (6) rHW-gal-9 (ER); (7) rHW-gal-9 (arrow); (8) rWW-gal-9 (ER); (9) rWW-gal-9 (arrow). (**B**) Haemagglutination results of rHW-gal-3 and rWW-gal-3. Parasite galectin was desalted and reconcentrated before testing, rHW-gal-3 (without lactose removal step) was used to compare the agglutination ability before and after desalting. The galectin buffer was used as a negative control. Desalted rHW-gal-3 was capable of haemagglutination at concentrations of 59.5 µg/mL and partial haemagglutination was visible at 29.75 µg/mL. rHW-gal-3 before desalting, displayed partial haemagglutination at ~237.5 µg/mL. rWW-gal-3 did not display hemagglutination at any of the tested concentrations.

3.4. Hemagglutination Assay

A hemagglutination assay using horse RBCs was used to also check carbohydrate binding. Galectins produced via Nickel-affinity did not agglutinate RBCs at 120 µg/mL (rHW-gal-9) or 60 µg/mL (rWW-gal-9), rHW-gal-3 and rWW-gal-3 displayed weak agglutination at 12 µg/mL (Supplementary Materials).

Lactose purified and desalted rHW-gal-3 displayed agglutination at 119.5 µg/mL and 59.5 µg/mL with some activity at 29.8 µg/mL, as recorded in Figure 7. Lactose inhibited the ability of rHW-gal-3 to agglutinate the RBC, as

shown by the sample of rHW-gal-3 in elution buffer. rWW-gal-3 did not agglutinate RBCs at the tested range of 65.5–8.2 µg/mL.

3.5. HCA-7 CRC Proliferation Assay

The HCA-7 CRC cell line was treated with nematode galectins for 24 h, with rHW-gal-3. rHW-gal-3 significantly increased the proliferation of HCA-7 CRC cells at 5 µg/mL, 2.5 µg/mL and 1.25 µg/mL compared to the control. This increase in proliferation was observed in 2 of the 3 batches of rHW-gal-3 made, as represented in Figure 8. HW-gal-9, WW-gal-3, and WW-gal-9 were likewise tested, but no significant differences in proliferation were identified.

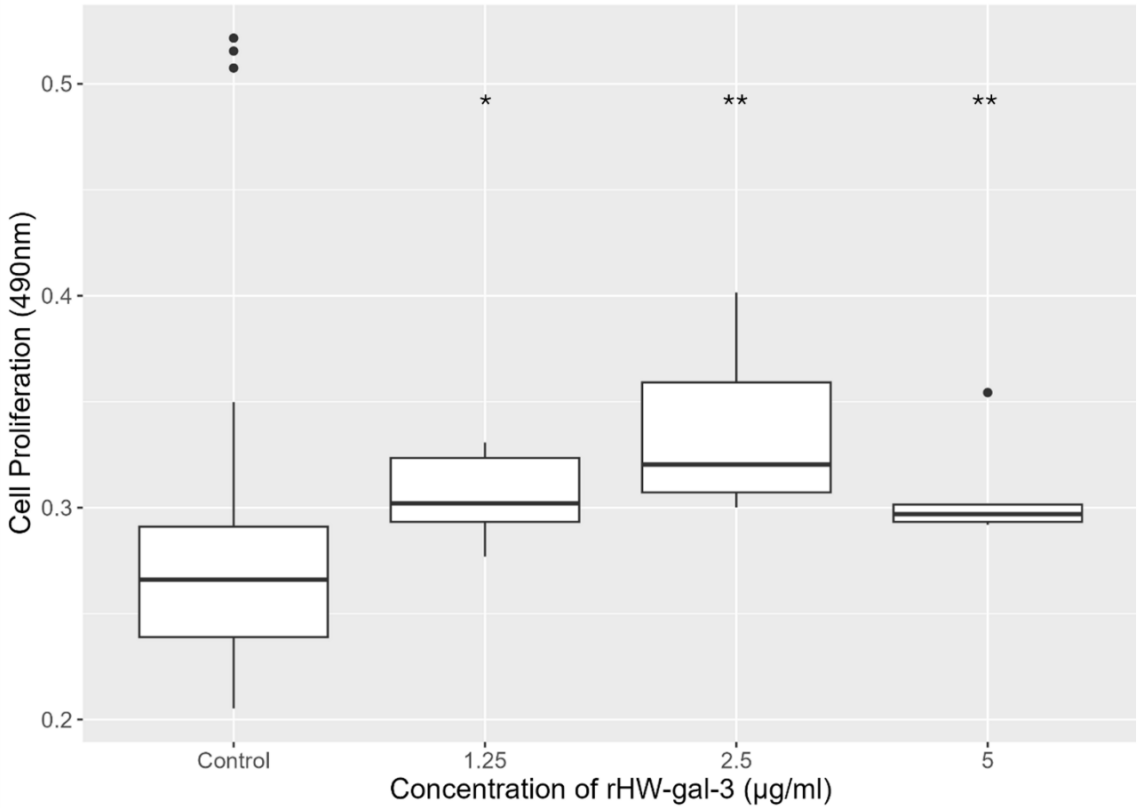

Figure 8. HCA-7 CRC cell proliferation after 24 h treatment with rHW-gal-3 or controls. Proliferation results from 7 proliferation assays using different rHW-gal-3 at 5 µg/mL, 2.5 µg/mL and 1.25 µg/mL. Significance was determined using Wilcoxon signed-rank test in reference to the control group, outliers are shown as points. Figure representative of one experiment but similar results were shown from n = 3 assays (* $p < 0.05$, ** $p < 0.01$).

3.6. Galectin-Binding to HCA-7 CRC

HCA-7 CRC cells treated with nickel-purified rWW-gal-9, showed a significant increase in the mean grey value (MGV) of the FITC stain, as shown in Figure 9, but not the DAPI stain which was used as a control for brightness fluctuations between images, indicating galectin binding after 72 h. HCA-7 CRC cells treated with the other galectins did not display any increased FITC stain that would indicate galectin binding, as shown by Figure 9.

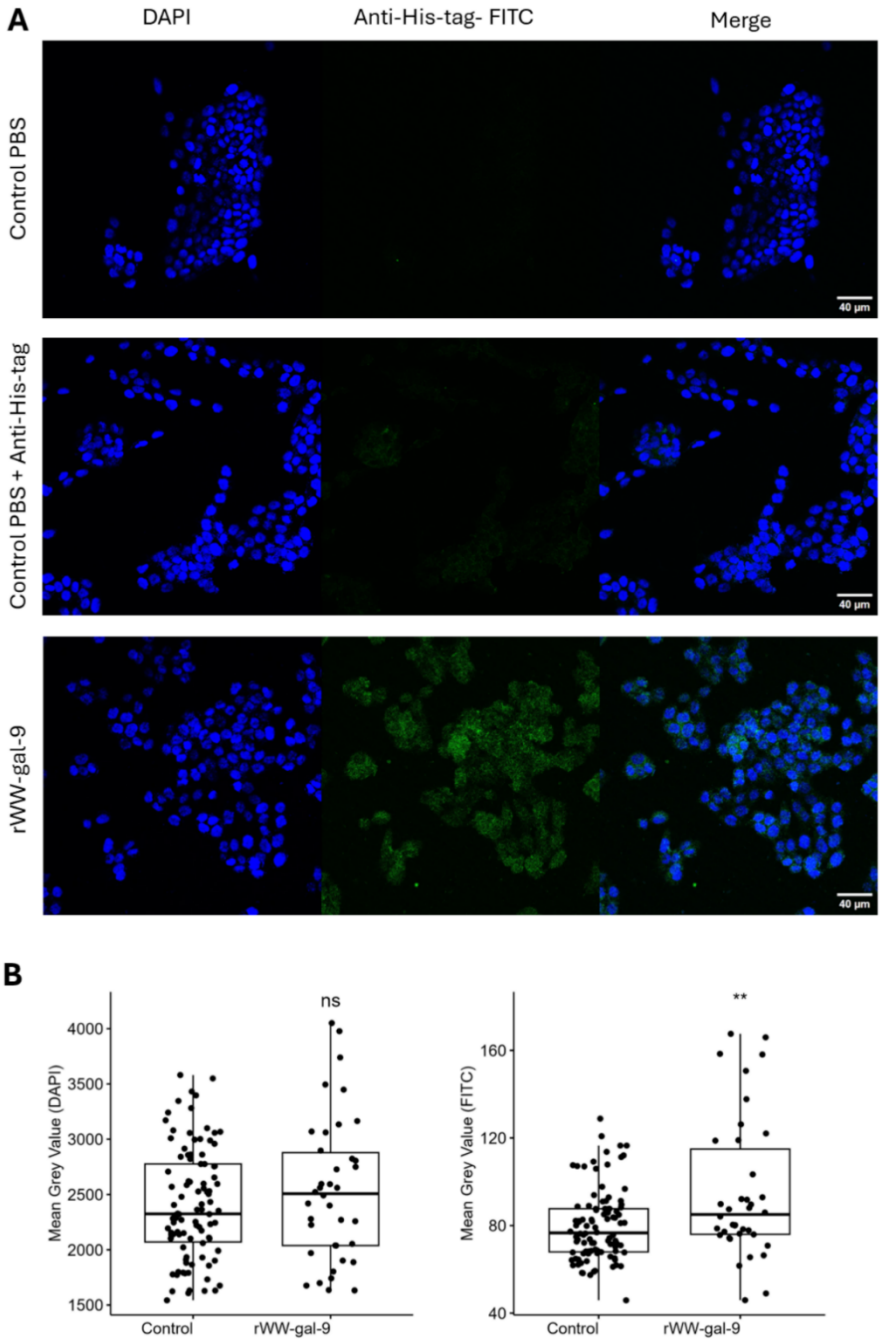

Figure 9. Binding of parasite galectins to HCA-7 CRC cells after 72 h. DAPI and FITC (Anti-His-tag-FITC conjugated antibody) channels and merged images (colour). (**A**) Control cells (DAPI stain only), control + His-tag (DAPI + anti-His-tag-FITC stain), rWW-gal-9 treated cells (DAPI + anti-His-tag-FITC stain). (**B**) MGV of DAPI and FITC channels of control cells (DAPI + anti-His-tag stain) compared to rWW-gal-9. The MGV of the cells treated with rWW-gal-9 had a nonsignificant change in the DAPI channel and a significant increase in the FITC channel (<0.05). Significance determined through unpaired *T*-test (** p <0.01).

4. Discussion

This study aimed to determine if the proteome and genome of hookworm and whipworm contained known protein sequences that could be homologs of human gal-3 and gal-9. Using proteome and genome sequencing data, several nematode galectins from *N. americanus* and *T. trichiura* were identified as potential homologs for human galectin-3 and galectin-9. Based on in-silico characterisation, four proteins were recombinantly expressed and purified via lactose bindings, suggesting isolation of active recombinant proteins. For the potential hookworm galectin-3 homolog (rHW-gal-3), it was observed to increase proliferation of epithelial cells, and agglutinate red blood cells. A galectin-9-like protein from *T. trichiura* was found to bind the epithelial cell line but this was not reflected in a change in proliferation.

When mining the nematode databases for potential human galectin-3 homologs, several protein sequences from Hookworm were identified, 11 contained binding residues with high similarity to human gal-3. In the whipworm genome/proteome, only 4 galectin-3 protein contained binding residues very similar to human gal-3. Based on structural and sequence similarity, rHW-gal-3 and rWW-gal-3 were selected for further analysis and protein expression. In-silico structural analysis predicted rHW-gal-3 is a prototype galectin, like human gal-3; it contains only one CRD but could form multimers. Interestingly, rWW-gal-3 is predicted to be a tandem galectin where the N-CRD of rWW-gal-3 resembled the CRD of human gal-3 in structure, and the C-CRD more closely resembled the C-CRD of human gal-9. In both nematode galectin-3 homologs, 2 key binding residues were different when aligned in Matchmaker; rHW-gal-3 had Lys^{46} in place of the $Arg^{144,}$ and rWW-gal-3 had Ser^{50} in place of Asn^{160}.

As both human gal-3 and gal-9 are potent immunomodulators, the potential immunoregulatory action of proteins that contain similar amino acids in the potential binding sites might be worth investigating.

In searching for potential galectin-9 homologs, 23 protein sequences from hookworm were analysed, with 10 containing potential binding residues with high similarity to human gal-9. In the whipworm genome, 8 galectin-9 like proteins were analysed, with 4 showing key binding residues of high similarity to human gal-9. Structural analysis predicted that rHW-gal-9 closely resembled human gal-9 in the N-CRD region and human gal-3 in the C-CRD region, although the C-CRD also resembled that of human gal-9.

There were several differences between the key binding residues of rHW-gal-9 and human gal-9, on the N-CRD, S^{63} was present in place of Asn^{62}. This substitution was recorded in the alignments of several papers reporting galectin-9 homologs [71,72]. On the C-CRD Lys^{181} in place of Asn^{253} and Asn^{183} in place of His^{255}, the predicted structure also showed misalignment on one of the turns in the pleat structure. When the C-CRD was compared to human gal-3 only one substitution was noted, Lys^{181} in place of Arg^{144}. Substitution of His^{255} on the C-CRD of human gal-9 for either Ala or Lys was also shared by the tandem parasite galectins, rHw-gal-9 and rWW-gal-9 and rWW-gal-3.

The selected sequences were processed again through BLAST, rHW-gal-9 returned 20 sequences from a variety of nematodes that had >85% similarity but an exact match was not found in the NCBI databases. This may indicate that rHW-gal-9-like-protiens are conserved across many nematode species, whereas highly similar sequences for rWW-gal-3 and rWW-gal-9 were only found in closely related worm species. It also indicated that the rHW-gal-9 sequence, as recorded by Logan et al. [34], may be too long, as the sequence alignments would begin at Met^{97}. Upon modelling of both untrimmed and trimmed protein the decision was made to trim the protein for expression to match the length of the other highly similar sequences [71,72].

Past research has identified rWW-gal-9 in embryonated whipworm eggs by Dixon et al. [73]. However, no work has been done to isolate the functions of either galectin beyond the assumption that they are immune signalling molecules [73]. While rHW-gal-9, has not been directly researched, there has been research into human gal-9 homologs in other species. *Toxascaris leonina* galectin-9 (Tl-gal-9) (GenBank: ARM19984.1), was observed to inhibit dextran sulphate sodium (DSS)-induced intestinal inflammation in mice after recombinant galectin injections [14]. This study showed that, compared to the diseased group that was untreated, Tl-gal-9 treated mice, had longer colons, were protected from the effects of DSS, and spleen lymphocytes expressed higher levels of IL-10 and TGF-β, and lowered expression of IL-4 and IFN-γ [14]. Gal-9 homologs with immunomodulatory effects have also been reported in *Brugia malayi* [72], galectin Bma-LEC-2, was able to induce macrophage polarisation to the alternatively activated macrophage (M2) phenotype and induce Th1 cell apoptosis. The substitution of Asparagine (N^{62}) in human gal-9, for Serine in the parasite galectin, was repeated across all of the parasite galectins shown, this was also present in *T. circ*-gal-1, tl-gal-9, and Bma-LEC-2 [14,72,74].

The galectin DNA sequences underwent minor changes to assist in their expression in *E. coli* compared to nematode systems. SDS-PAGE results showed that the proteins initially expressed very well in *E. coli.* However further refinement of the method was required to maintain protein stability in solution, and 3 batches of galectin were produced over the course of this research. Initially, the galectins were purified using Nickel-affinity chromatography to select for the 6XHis-tag, and a large quantity of galectin was produced using this method, however variance in proliferation of HCA-7 cells between batches produced with this method, and haemagglutination assays indicated the carbohydrate-binding activity of this galectin was low (Supplementary Materials). This was replaced with using lactose-affinity purification to maximise the amount of recovered galectin with an active CRD and remove any non-lactose-binding proteins. SDS-PAGE showed that the galectin recovered using lactose-affinity had carbohydrate binding activity, but yield for rHW-gal-9, rWW-gal-3 and r-WW-gal-9 was too low to use in replicate proliferation and immunolocalisation assays.

In vitro assays indicated that the recombinant nematode galectins were capable of interacting with mammalian cells. rHW-gal-3 could significantly alter the proliferation HCA-7 CRC cells at concentrations

between 1.25 µL/mL and 5 µg/mL, however other recombinant galectins did not have significant effects on proliferation. An increase in proliferation of HCA-7 CRC cells following galectin treatment is corroborated by research into the *Strongyloides ratti* galectin, and *Trichuris* infections [75,76]. Researchers found that human epithelial colorectal adenocarcinoma cells (Caco2) with a simulated wound that were treated with the galectin displayed faster wound closure compared to untreated cells [75].

Galectin-treated HCA-7 CRC cells were visualised using microscopy. Of these, rWW-gal-9 showed binding, measured by the MGV of the FITC stain, compared to the control. While rHW-gal-3 had significant effects on proliferation, cell surface binding was not observed. This could be due to the timepoint selected for the experiment, or the effect not being caused by direct galectin-cell binding. There was a large degree of variation in the brightness of the images taken during this experiment, this may be due to imaging the cells at 40× magnification. To accommodate this the MGV of the DAPI stain was used to determine if brightness was variable between samples, despite sampling several images per galectin, which was apparent in all galectins but rWW-gal-9. Nematode galectin has been recorded as facilitating larval invasion of the gut mucosa and binding to epithelial cells in *T. spiralis* infections [77].

Haemagglutination assay further indicated that rHW-gal-3 has a functional CRD region as it was able to form an RBC "mesh" at high concentrations, but agglutination was inhibited when lactose was present. However, rWW-gal-3 was unable to agglutinate RBCs at the concentrations tested, which may be caused by the galectin possessing low specificity for horse blood groups or that the concentration was too low to cause agglutination [78,79].

This study has 3 main limitations. Firstly, the sequences were collected from 3 different online databases, but the sequences were from only 3 different sources, limiting our ability to cross reference sequences for accuracy. All the *T. trichiura* sequences were from one source and all the *N. americanus* sequences were from two sources [34,36,80]. It is a possibility that some other sequences recorded in the online databases have been translated incorrectly or incompletely [39]. Secondly, a large portion of the bioinformatics section focuses on the use of Matchmaker and Alphafold which rely on the predicted structure of a protein based on the protein sequence. This has a level of inaccuracy, as the predicted models may contain regions modelled with low confidence. Lastly, the results of in-vitro assays displayed a large variance between replicates, this could be due to galectin activity decreasing somewhat after long-term storage at 4 °C, or low carbohydrate binding in nickel-purified galectins. The method was altered in subsequent batches to prioritise recovering galectin with lactose-affinity and was stored with lactose at −80 °C and desalted as required [52]. This inconsistency and loss of activity between batches and following long term storage is common among recombinantly produced galectins [52].

In summary, 2 potential gal-9 and gal-3 nematode human homologs were synthesised from the proteomes of *N. americanus* and *T. trichiura*. Two of the tandem parasite homologs, rWW-gal-3 and rHW-gal-9, were found to have CRD regions resembling both human gal-3 and gal-9. The galectins were successfully expressed and found to have carbohydrate binding capabilities, binding to lactose. Furthermore, rHW-gal-3 caused significant increases in HCA-7 CRC cell proliferation in culture, suggesting the galectin interferes with host processes. Future research will focus on the effects of rHW-gal-3 on immune cells and cytokine production and compare the activity to human-gal-3 and gal-9.

Supplementary Materials

The additional data and information can be downloaded at: https://media.sciltp.com/articles/others/25121816 47232947/ParSci-25110006-Supplementary-Material-FC-done.pdf.

Author Contributions

E.M.: writing—original draft preparation, methodology, conceptualization, investigation, visualisation, formal analysis; G.Z.: methodology, writing—reviewing and editing, writing—original draft preparation, resources; F.A.-N.: writing—reviewing and editing, supervision, resources; T.B.: writing—reviewing and editing, methodology, resources; D.P.: Supervision, writing—reviewing and editing; S.P.: supervision, methodology, conceptualization, writing—reviewing and editing. All authors have read and agreed to the published version of the manuscript.

Funding

This research received a Health Innovation and Transformation Centre (HITC) early career researcher seed grant from Federation University. This research was supported by an Australian Government Research Training Program (RTP) Scholarship doi.org/10.82133/C42F-K220.

Institutional Review Board Statement

Not Applicable.

Informed Consent Statement

Not Applicable.

Data Availability Statement

Data will be available at a request from the corresponding author.

Conflicts of Interest

The Authors declare no conflict of interest.

Use of AI and AI-Assisted Technologies

During the preparation of this work, the authors used AlphaFold to model the predicted structure of proteins based on sequence. After using this tool/service the authors reviewed and edited the content as needed and take full responsibility for the content of the published article.

References

1. Barnig, C.; Bezema, T.; Calder, P.C.; et al. Activation of resolution pathways to prevent and fight chronic inflammation: Lessons from asthma and inflammatory bowel disease. *Front. Immunol.* **2019**, *10*, 1699.
2. Furman, D.; Campisi, J.; Verdin, E.; et al. Chronic inflammation in the etiology of disease across the life span. *Nat. Med.* **2019**, *25*, 1822–1832.
3. Wylezinski, L.S.; Gray, J.D.; Polk, J.B.; et al. Illuminating an invisible epidemic: A systemic review of the clinical and economic benefits of early diagnosis and treatment in inflammatory disease and related syndromes. *J. Clin. Med.* **2019**, *8*, 493.
4. Dyndor, K.; Golec, K.; Ruchala, M.; et al. Organ and prenatal toxicity of nonsteroidal anti-inflammatory drugs. *Curr. Issues Pharm. Med. Sci.* **2015**, *28*, 200–203.
5. Ryan, S.M.; Ruscher, R.; Johnston, W.A.; et al. Novel antiinflammatory biologics shaped by parasite–host coevolution. *Proc. Natl. Acad. Sci. USA* **2022**, *119*, e2202795119.
6. Fleming, J.O.; Weinstock, J.V. Clinical trials of helminth therapy in autoimmune diseases: Rationale and findings. *Parasite Immunol.* **2015**, *37*, 277–292.
7. Ryan, S.M.; Eichenberger, R.M.; Ruscher, R.; et al. Harnessing helminth-driven immunoregulation in the search for novel therapeutic modalities. *PLoS Pathog.* **2020**, *16*, e1008508.
8. Gazzinelli-Guimaraes, P.H.; Nutman, T.B. Helminth parasites and immune regulation. *F1000Res* **2018**, *7*, 1685.
9. Pierce, D.R.; McDonald, M.; Merone, L.; et al. Effect of experimental hookworm infection on insulin resistance in people at risk of Type 2 Diabetes: A randomized, placebo-controlled trial. *medRxiv* **2023**. https://doi.org/10.1101/2023.03.16.23287372.
10. Croese, J.; Gaze, S.T.; Loukas, A. Changed gluten immunity in celiac disease by Necator americanus provides new insights into autoimmunity. *Int. J. Parasitol.* **2013**, *43*, 275–282.
11. Harnett, W. Secretory products of helminth parasites as immunomodulators. *Mol. Biochem. Parasitol.* **2014**, *195*, 130–136.
12. Stear, M.; Preston, S.; Piedrafita, D.; et al. The Immune Response to Nematode Infection. *Int. J. Mol. Sci.* **2023**, *24*, 2283.
13. Goodridge, H.S.; Marshall, F.A.; Wilson, E.H.; et al. *In vivo* exposure of murine dendritic cell and macrophage bone marrow progenitors to the phosphorylcholine-containing filarial nematode glycoprotein ES-62 polarizes their differentiation to an anti-inflammatory phenotype. *Immunology* **2004**, *113*, 491–498.
14. Kim, J.Y.; Cho, M.K.; Choi, S.H.; et al. Inhibition of dextran sulfate sodium (DSS)-induced intestinal inflammation via enhanced IL-10 and TGF-β production by galectin-9 homologues isolated from intestinal parasites. *Mol. Biochem. Parasitol.* **2010**, *174*, 53–61.
15. Karabowicz, J.; Długosz, E.; Bąska, P.; et al. Nematode Orthologs of Macrophage Migration Inhibitory Factor (MIF) as Modulators of the Host Immune Response and Potential Therapeutic Targets. *Pathogens* **2022**, *11*, 258.
16. Brinchmann, M.F.; Patel, D.M.; Iversen, M.H. The role of galectins as modulators of metabolism and inflammation. *Mediat. Inflamm.* **2018**, *2018*, 9186940.
17. Donskow-Łysoniewska, K.; Maruszewska-Cheruiyot, M.; Stear, M. The interaction of host and nematode galectins influences the outcome of gastrointestinal nematode infections. *Parasitology* **2021**, *148*, 648–654.

18. Varki, A.; Cummings, R.D.; Esko, J.D.; et al. *Essentials of Glycobiology [Internet]*; Cold Spring Harbor Laboratory Press: Woodbury, NY, USA, 2015.
19. Mukai, K.; et al. IgE and Mast Cells in Host Defense against Parasites and Venoms. In *Seminars in Immunopathology*; Springer: Berlin/Heidelberg, Germany, 2016; Volume 38, pp. 581–603.
20. Albert-Bayo, M.; Paracuellos, I.; González-Castro, A.M.; et al. Intestinal mucosal mast cells: Key modulators of barrier function and homeostasis. *Cells* **2019**, *8*, 135.
21. Zhu, C.; Anderson, A.C.; Schubart, A.; et al. The Tim-3 ligand galectin-9 negatively regulates T helper type 1 immunity. *Nat. Immunol.* **2005**, *6*, 1245–1252.
22. Wu, C.; Thalhamer, T.; Franca, R.F.; et al. Galectin-9-CD44 interaction enhances stability and function of adaptive regulatory T cells. *Immunity* **2014**, *41*, 270–282.
23. Chen, X.; Song, C.H.; Liu, Z.Q.; et al. Intestinal epithelial cells express galectin-9 in patients with food allergy that plays a critical role in sustaining allergic status in mouse intestine. *Allergy* **2011**, *66*, 1038–1046.
24. Nagae, M.; Nishi, N.; Murata, T.; et al. Crystal structure of the galectin-9 N-terminal carbohydrate recognition domain from Mus musculus reveals the basic mechanism of carbohydrate recognition. *J. Biol. Chem.* **2006**, *281*, 35884–35893.
25. Yoshida, H.; Teraoka, M.; Nishi, N.; et al. X-ray structures of human galectin-9 C-terminal domain in complexes with a biantennary oligosaccharide and sialyllactose. *J. Biol. Chem.* **2010**, *285*, 36969–36976.
26. Saraboji, K.; Håkansson, M.; Genheden, S.; et al. The carbohydrate-binding site in galectin-3 is preorganized to recognize a sugarlike framework of oxygens: Ultra-high-resolution structures and water dynamics. *Biochemistry* **2012**, *51*, 296–306.
27. Díaz-Alvarez, L.; Ortega, E. The many roles of galectin-3, a multifaceted molecule, in innate immune responses against pathogens. *Mediat. Inflamm.* **2017**, *2017*, 9247574.
28. Farhadi, S.A.; Liu, R.; Becker, M.W.; et al. Physical tuning of galectin-3 signaling. *Proc. Natl. Acad. Sci. USA* **2021**, *118*, e2024117118.
29. Chen, H.Y.; Sharma, B.B.; Yu, L.; et al. Role of galectin-3 in mast cell functions: Galectin-3-deficient mast cells exhibit impaired mediator release and defective JNK expression. *J. Immunol.* **2006**, *177*, 4991–4997.
30. Donskow-Łysoniewska, K.; Maruszewska-Cheruiyot, M.; Krawczak-Wójcik, K.; et al. Nematode galectin binds IgE and modulates mast cell activity. *Vet. Parasitol.* **2022**, *311*, 109807.
31. Bauters, L.; Naalden, D.; Gheysen, G. The distribution of lectins across the phylum nematoda: A genome-wide search. *Int. J. Mol. Sci.* **2017**, *18*, 91.
32. Ilic, N.; Bojic-Trbojevic, Z.; Lundström-Stadelmann, B.; et al. Immunomodulatory components of Trichinella spiralis excretory-secretory products with lactose-binding specificity. *EXCLI J.* **2022**, *21*, 793.
33. Lu, M.M.; Tian, X.W.; Yang, X.C.; et al. The N- and C-terminal carbohydrate recognition domains of Haemonchus contortus galectin bind to distinct receptors of goat PBMC and contribute differently to its immunomodulatory functions in host-parasite interactions. *Parasites Vectors* **2017**, *10*, 409.
34. Logan, J.; Pearson, M.S.; Manda, S.S.; et al. Comprehensive analysis of the secreted proteome of adult Necator americanus hookworms. *PLoS Negl. Trop. Dis.* **2020**, *14*, e0008237.
35. Foth, B.J.; Tsai, I.J.; Reid, A.J.; et al. Whipworm genome and dual-species transcriptome analyses provide molecular insights into an intimate host-parasite interaction. *Nat. Genet.* **2014**, *46*, 693–700.
36. Mitreva, M.; Abubucker, S.; Martin, J.; et al. *Direct Submission-Genome of Necator Americanus*; National Library of Medicine (The Genome Institute, Washington University School of Medicine): St. Louis, MO, USA, 2013.
37. Altschul, S.F.; Gish, W.; Miller, W.; et al. Basic local alignment search tool. *J. Mol. Biol.* **1990**, *215*, 403–410.
38. Bateman, A.; Martin, M.-J.; Orchard, S.; et al. UniProt: The universal protein knowledgebase in 2023. *Nucleic Acids Res.* **2022**, *51*, D480–D489.
39. UniProt Consortium. UniProt: The universal protein knowledgebase in 2021. *Nucleic Acids Res.* **2021**, *49*, D480–D489.
40. Camacho, C.; Coulouris, G.; Avagyan, V. BLAST+: Architecture and applications. *BMC Bioinform.* **2009**, *10*, 421.
41. Tamura, K.; Stecher, G.; Kumar, S. MEGA11: Molecular evolutionary genetics analysis version 11. *Mol. Biol. Evol.* **2021**, *38*, 3022–3027.
42. Waterhouse, A.M.; Procter, J.B.; Martin DM, A.; et al. Jalview Version 680 2—A multiple sequence alignment editor and analysis workbench. *Bioinformatics* **2009**, *25*, 1189–1681.
43. Kalyaanamoorthy, S.; Minh, B.Q.; Wong, T.K.F.; et al. ModelFinder: Fast model selection for accurate phylogenetic estimates. *Nat. Methods* **2017**, *14*, 587–589.
44. Hoang, D.T.; Chernomor, O.; Von Haeseler, A.; et al. UFBoot2: Improving the ultrafast bootstrap approximation. *Mol. Biol. Evol.* **2018**, *35*, 518–522.
45. Nguyen, L.-T.; Schmidt, H.A.; Von Haeseler, A.; et al. IQ-TREE: A fast and effective stochastic algorithm for estimating maximum-likelihood phylogenies. *Mol. Biol. Evol.* **2015**, *32*, 268–274.
46. Minh, B.Q.; Schmidt, H.A.; Chernomor, O.; et al. IQ-TREE 2: New models and efficient methods for phylogenetic inference in the genomic era. *Mol. Biol. Evol.* **2020**, *37*, 1530–1534.

47. Jumper, J.; Evans, R.; Pritzel, A.; et al. Highly accurate protein structure prediction with AlphaFold. *Nature* **2021**, *596*, 583–589.
48. Pettersen, E.F.; Goddard, T.D.; Huang, C.C.; et al. UCSF ChimeraX: Structure visualization for researchers, educators, and developers. *Protein Sci.* **2021**, *30*, 70–82.
49. Rehbein, P.; Berz, J.; Kreisel, P.; et al. "CodonWizard"—An intuitive software tool with graphical user interface for customizable codon optimization in protein expression efforts. *Protein Expr. Purif.* **2019**, *160*, 84–93.
50. Sakthivel, D.; Littler, D.; Shahine, A.; et al. Cloning, expression, purification and crystallographic studies of galectin-11 from domestic sheep (*Ovis aries*). *Struct. Biol. Cryst. Commun.* **2015**, *71*, 993–997.
51. Sambrook, J.; Russell, D.W. The Hanahan Method for Preparation and Transformation of Competent *E. coli*: High-efficiency Transformation. *CSH Protoc* **2006**, *2006*, pdb. prot3942.
52. Wu, S.C.; Paul, A.; Ho, A.; et al. Generation and Use of Recombinant Galectins. *Curr. Protoc.* **2021**, *1*, e63.
53. Mouradov, D.; Sloggett, C.; Jorissen, R.N.; et al. Colorectal cancer cell lines are representative models of the main molecular subtypes of primary cancer. *Cancer Res.* **2014**, *74*, 3238–3247.
54. RStudio Team. *RStudio: Integrated Development for R*; RStudio Team: Boston, MA, USA, 2020.
55. Prato, C.A.; Carabelli, J.; Cattaneo, V.; et al. Purification of Recombinant Galectins Expressed in Bacteria. *STAR Protoc.* **2020**, *1*, 100204.
56. R Core Team. *R: A Language and Environment for Statistical Computing*; R Foundation for Statistical Computing: Vienna, Austria, 2023.
57. Xu, S.; Chen, M.; Feng, T.; et al. Use ggbreak to Effectively Utilize Plotting Space to Deal with Large Datasets and Outliers. *Front. Genet.* **2021**, *12*, 774846.
58. Aphalo, P.J. ggpmisc: Miscellaneous Extensions to 'ggplot2' 2025. Available online: https://cran.r-project.org/web/packages/ggpmisc/ggpmisc.pdf (accessed on 22 October 2025).
59. Aphalo, P.J. ggpp: Grammar Extensions to 'ggplot2' 2024. Available online: https://github.com/aphalo/ggpp (accessed on 22 October 2025).
60. Kassambara, A. ggpubr: 'ggplot2' Based Publication Ready Plots. 2023. Available online: https://CRAN.R-project.org/package=ggpubr (accessed on 22 October 2025).
61. Wilke, C.O.; Wiernik, B.M. ggtext: Improved Text Rendering Support for 'ggplot2' 2022. Available online: https://CRAN.R-project.org/package=ggtext (accessed on 22 October 2025).
62. Xie, Y. *knitr: A Comprehensive Tool for Reproducible Research in R*; Chapman and Hall/CRC: Boca Raton, FL, USA, 2014.
63. Schauberger, P.; Walker, A. Openxlsx: Read, Write and Edit xlsx Files 2025. Available online: https://CRAN.R-project.org/package=openxlsx (accessed on 22 October 2025).
64. Lemon, J. Plotrix: A package in the red light district of R. *R News* **2006**, *6*, 8–12.
65. Xie, Y.; Allaire, J.J.; Grolemund, G. R Markdown: The Definitive Guide. Chapman and Hall/CRC: Boca Raton, FL, USA, 2018.
66. Allaire, J.J.; Xie, Y.; Dervieux, C.; et al. rmarkdown: Dynamic Documents for R. 2024. Available online: https://CRAN.R-project.org/package=rmarkdown (accessed on 22 October 2025).
67. Xie, Y.; Dervieux, C.; Riederer, E. R Markdown Cookbook. Chapman and Hall/CRC: Boca Raton, FL, USA, 2020.
68. Kassambara, A. Rstatix: Pipe-Friendly Framework for Basic Statistical Tests 2023. Available online: https://cir.nii.ac.jp/crid/1360864422589421952 (accessed on 22 October 2025).
69. Johnston, B. standard: Simplified Fitting and Use of Standard Curves 2025. Available online: https://bradyajohnston.github.io/standard/index.html (accessed on 22 October 2025).
70. Wickham, H.; Averick, M.; Bryan, J.; et al. Welcome to the Tidyverse. *J. Open Source Softw.* **2019**, *4*, 1686.
71. Ha, M.S.; Han, C.W.; Jeong, M.S.; et al. Structures of W77F/W212F and W77F/W212F Toxascaris leonine galectin complex with glucose. *Carbohydr. Res.* **2025**, *558*, 109657.
72. Loghry, H.J.; Sondjaja, N.A.; Minkler, S.J.; et al. Secreted filarial nematode galectins modulate host immune cells. *Front. Immunol.* **2022**, *13*, 952104.
73. Dixon, H.; Johnston, C.; Else, K. Antigen selection for future anti-Trichuris vaccines: A comparison of cytokine and antibody responses to larval and adult antigen in a primary infection. *Parasite Immunol.* **2008**, *30*, 454–461.
74. Hafidi, N.N.; Swan, J.; Faou, P.; et al. Teladorsagia Circumcincta Galectin-Mucosal Interactome in Sheep. *Vet. Sci.* **2021**, *8*, 216.
75. Ditgen, D.; Anandarajah, E.M.; Reinhardt, A.; et al. Comparative characterization of two galectins excreted-secreted from intestine-dwelling parasitic versus free-living females of the soil-transmitted nematode Strongyloides. *Mol. Biochem. Parasitol.* **2018**, *225*, 73–83.
76. Klementowicz, J.E.; Travis, M.A.; Grencis, R.K. Trichuris muris: A model of gastrointestinal parasite infection. *Semin. Immunopathol.* **2012**, *34*, 815–828.

77. Ma, K.N.; Zhang, Y.; Zhang, Z.Y.; et al. *Trichinella spiralis* galectin binding to toll-like receptor 4 induces intestinal inflammation and mediates larval invasion of gut mucosa. *Vet. Res.* **2023**, *54*, 113.
78. Gasson, R.; Roper, J.A.; Slack, R.J. A Quantitative Human Red Blood Cell Agglutination Assay for Characterisation of Galectin Inhibitors. *Int. J. Mol. Sci.* **2024**, *25*, 6756.
79. Xu, J.; Yang, F.; Yang, D.Q.; et al. Molecular characterization of Trichinella spiralis galectin and its participation in larval invasion of host's intestinal epithelial cells. *Vet. Res.* **2018**, *49*, 79.
80. Foth, B.J.; Tsai, I.J.; Reid, A.J.; et al. The whipworm genome and dual-species transcriptomics of an intimate host-pathogen interaction. *Nat. Genet.* **2014**, *46*, 693–700.